TIME FRAME MEASUREMENTS IMPACT ON PROBABILISTIC BEHAVIOUR OF PHOTOVOLTAIC SYSTEMS

Professor **Giuseppe Marco TINA**[1], Professor **Gilles NOTTON**[2], Lecturer **Ciprian NEMES**[3]

[1]University of Catania, Italy, [2]University of Corsica, France
[3]Technical University of Iasi, Romania

REZUMAT. Pentru un sistem electric cu panouri fotovoltaice este important să se evalueze şi să se înţeleagă modul în care intervalele de măsură a radiaţiei solare pot afecta capacitatea sistemului de a genera şi de a acoperi necesarul de sarcină. Nivelul puterii generat de un sistem fotovoltaic se evaluează pe baza valorilor medii orare ale gradului de nebulozitate. Obiectivul principal al acestei lucrări este de a evalua efectele diferitelor intervale de măsură a radiaţiei solare asupra indicatorilor de adecvabilitate ai unui sistem ce integrează surse fotovoltaice.

Cuvinte cheie: energie solară, nebulozitate orară, indicatori de adecvabilitate.

ABSTRACT. For a generation system including photovoltaic systems is important to assess and understand how different time frames for the irradiation measurements can impact the ability of the system generating capacity to meet the total system load. The electrical output power generated by a photovoltaic system is evaluated using the hourly average clearness index values. The main objective of this paper is to evaluate the effects of different time frames, over that the measurement data are recorded, on the probabilistic behaviour of a grid-connected photovoltaic system.

Key words: solar energy, hourly clearness index, adequacy indices.

1. INTRODUCTION

During the last decades, a growing interest in renewable energy resources has been observed. Even if electric energy from renewable energy sources brings various benefits to power system, due to the variable and intermittent behaviour of many renewable resources, their integration into electric grid leads to new challenges in the system operation.

The operation of power systems with renewable energy sources, such as photovoltaic systems, has to consider the stability of the electrical power system, which is based on a reliable power generation that is permanently balanced by the load. Due the variation of the demanded load or the generated power by non-programmable generation units, for system balancing, the Independent System Operator (ISO) has to buy energy resources on the ancillary services markets. The relevant time for these markets is about 15 minutes, whereas the energy markets work on an hourly base. Therefore, for a generation system including photovoltaic systems, to evaluate the real energy needs is important to assess and understand how different time frames from the irradiation measurements can impact on power system adequacy. The adequacy associated to a generation power system is a measure of the ability of system generating capacity to meet the total system load.

Thus, our study is conducted in order to find the main adequacy indices, associated to a grid-connected photovoltaic system. Generally, the electrical output power generated by a photovoltaic system is evaluated using the hourly clearness index values. The main objective of this paper is to evaluate the effects of intra-hourly time frames, over that the measurement data are recorded, on the photovoltaic system adequacy indices over a long time interval.

The paper is organized as follows. In order to evaluate the adequacy indices, a brief description of the evaluation technique used in the paper is presented in section 2. Furthermore, the probability density functions associated to electrical output power and to load demand are also presented in this section, highlighting the main parameters that affect these functions. In section 3, a measurement database over 10 minutes time frame is analysed and involved in order to develop another two database, over 30 and 60 minutes time frames. Furthermore, these three database over mentioned time frames are involved in statistical analyses related to evaluate the upper, average and lower values of clearness index. In section 4 a numerical analysis is developed in order to calculate the adequacy indices, based on the 10, 30 and 60 minutes time frames and three scenarios related to load profile. Finally, the main conclusions are given in section 5.

2. GENERATING SYSTEM ADEQUACY

The adequacy associated to a generating power system is a measure of the ability of the system generating capacity to satisfy the total system load. Generally, the generating system adequacy evaluation process, focuses only on the balance between generating capacity and demanded load. The most common indices used for generating system adequacy evaluation are the Loss of Load Expectation (LOLE) and the Loss of Energy Expectation (LOEE) [1],[2]. LOLE [hours/year] indicates the average number of hours in a given period (usually one year) in which the hourly load is expected to exceed the available generating capacity. LOEE [MWh/year], sometimes known as the Expected Energy Not Supplied (EENS), specifies the expected energy that won't be supplied by the generation system due to those occasions when the demanded load exceeds the available generating capacity.

The basic approach to evaluate the adequacy of a generating system consists in development of two probabilistic models: a capacity model and a load model. Then, the capacity and load models are convolved to create a system's reserve margin variable, defined as the difference between the available capacity and the demanded load. The adequacy indices can be obtained by observing the available system's reserve margin variable. A positive reserve denotes that the system generation is sufficient to meet the system load, while a negative margin implies that the system load is not served.

Probabilistic model of photovoltaic system's output power. The electrical output power of a photovoltaic system depends on many factors, including the environmental conditions associated to the placement's site. An important factor that affects the value of electrical output power generated by a photovoltaic system is the clearness index value. This index provides information concerning the real amount of solar radiation falling on the earth surface compared with the available extraterrestrial solar radiation. Actually, the estimation of this index requires the solar data measurements.

The present paper is developed based on the analytical expression of probability density function of electrical output power generated by a photovoltaic system. In [3],[4],[5] detailed analytical approaches are developed based on the analytical relation between the photovoltaic output power and the irradiation level, and also on the probability density function of clearness index proposed by Holland and Huget [6]. Thus, the probability density function of monthly hourly output power of a photovoltaic system can be expressed as follows:

$$f_{P_{m,j}}\left(P_{m,j}\right)=\begin{cases}\dfrac{C_{m,j}\left(k_{tu}-\dfrac{\alpha_{m,j}\pm\Delta_{m,j}}{2}\right)}{\mp k_{tu}\cdot A_c\cdot\eta_{m,j}\cdot T'_{m,j}\cdot\Delta_{m,j}}\cdot e^{\frac{\lambda_{m,j}}{2}\left(\alpha_{m,j}\pm\Delta_{m,j}\right)}, & for \quad P_{m,j}\in\left[0,P(k_{tu})\right]\\ 0 & otherwise\end{cases} \quad (1)$$

where: $\Delta_{m,j}\left(P_{m,j}\right)=\sqrt{\alpha_{m,j}^2-\dfrac{4\cdot P_{m,j}}{\eta_{m,j}\cdot T'_{m,j}\cdot A_c}}$; $\alpha_{m,j}=\dfrac{T_{m,j}}{T'_{m,j}}$; $T_{m,j}, T'_{m,j}$ are some parameters used in solar irradiation evaluation; $C_{m,j}$ and $\lambda_{m,j}$ are the Holland and Huget distribution parameters; plus/minus signs is used for $T_{m,j}>0$ and $T'_{m,j}<0$, respectively $T_{m,j}>0$ and $T'_{m,j}\geq 0$.

More details and expressions of parameters involved in the probability density function are reported in [3],[4]. The appearance frequencies of monthly hourly values of output power are affected by the values of hourly clearness index, distributed in accordance with Holland and Huget [6]. In this distribution the variables that affect the probability density function values are only upper and average values of hourly clearness index, values that will be evaluated, for our database, in section 3.

Probabilistic model of load profile. The demanded load in power system is variable in time. There is no one unique profile or mathematical equation that can be adopted to represent the load characteristic curve. Thus, three different models related to load profile have been adopted in this paper. One of them has a smooth profile, having the same values of load for all hours of day, the second one is considered to be a smooth profile but only for daily hours, and the last one has a peak profile, with a maximum value on the midday. For hourly load values, a uniformly distributed function is adopted, with a given standard deviation around to average value of the hourly load. Thus, the probability density function of the hourly load, L_j, can be expressed as follows:

$$f(L_j)=\begin{cases}\dfrac{1}{L_{j_{\max}}-L_{j_{\min}}} & for\ L_j\in\left[L_{j_{\min}},L_{j_{\max}}\right]\\ 0 & otherwise\end{cases} \quad (2)$$

with $L_{j_{\max/\min}}=\bar{L}_j\pm\sqrt{3}\cdot\sigma$, where $\bar{L}_j$ is the hourly average load, σ is the standard deviation of load, and plus/minus sign is used for maximum/minimum load value, respectively.

3. SOLAR MEASUREMENTS DATABASE

The solar data used in this paper has been recorded over 10 minutes interval on the "Systèmes Physiques de l'Environnement" Laboratory, Ajaccio, (Corsica, France), the recorded data covering the period between 1999 and 2003. The meteorological station is located on Mediterranean seaside, at 41°55' north latitude, 8°48' east longitude and 75 m above the sea level. More details about the meteorological station and the instruments used to record the database can be found in [7],[8],[9].

This section focuses on some analyses of hourly clearness index values recorded over different time frame intervals. The measurements available in the original database are related, among others, to global and beam radiations, and also to clearness index. The database is characterized by 10 minutes acquisition intervals, thus the original database has collected and recorded six values for each hour of the day. Thus, in the paper, 37230 data of clearness index have been used for each year over the whole five years period.

Therefore, the clearness index values over 10, 30 and 60 minutes time frames have been drawn out and involved in a database transformation. Thus, each data from 30 and 60 minutes time frame have been evaluated as the average value of measured values during the time frame. Then, the database have been analysed in order to evaluate the upper, average and lower values over the whole period under study.

Figures 1-3 present the evolution of the upper, average and lower values of the hourly clearness index, for summer and winter solstices months (June and December) and for spring and autumn equinoxes months (March and September), respectively.

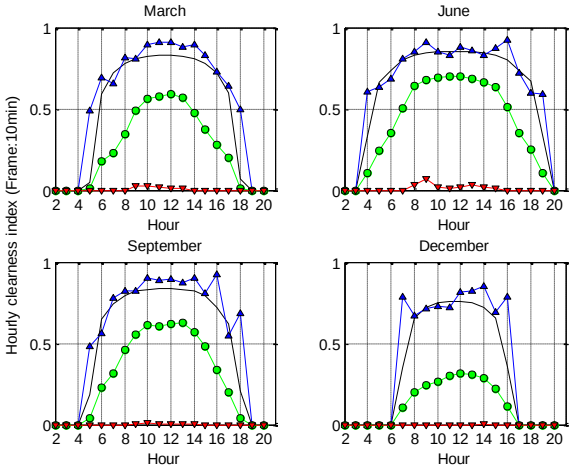

Fig. 1. Hourly clearness index measured values (▲: upper, •: average, ▼: lower) and clearness index (□) in clear sky condition, for 10 min time frame interval

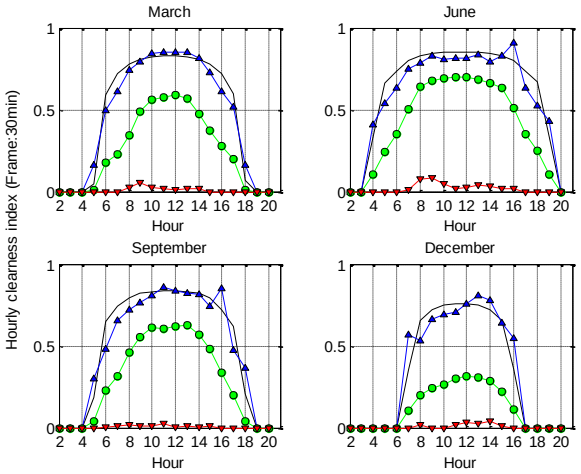

Fig. 2. Hourly clearness index measured values (▲: upper, •: average, ▼: lower) and clearness index (□) in clear sky condition, for 30 min time frame interval

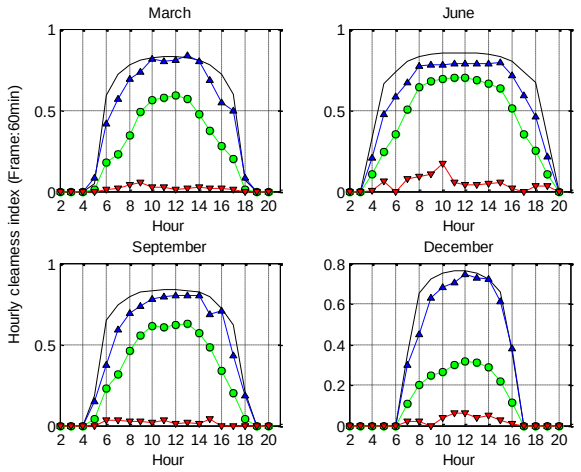

Fig. 3. Hourly clearness index measured values (▲: upper, •: average, ▼: lower) and clearness index (□) in clear sky condition, for 60 min time frame interval

In order to have a reference of measured values from original database, the ESRA model [10],[11] has been involved to evaluate the values of global and beam radiations in the hypothesis of clear sky condition. Figure 4 presents a comparison between hourly values of measured global and beam radiations with those from clear sky model, two analyses into orthogonal and horizontal planes being conducted. For instance, for the 204th day of the year, the global and beam radiations are drawn in the same diagram, and then with those from clear sky model. It has been considered the 204th day of year because that day has a specific profile, namely before noon has an almost a clear sky profile, while in the afternoon is a relatively cloudy sky.

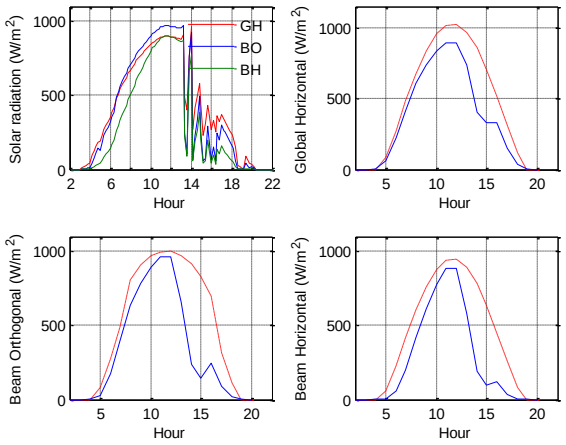

Fig. 4. Comparison between global and beam radiations with corresponding values in clear sky condition (for 204th day)

From Figures 1-3, especially for 10 minutes time frame database, it can be observed that many upper values of clearness index exceed the values of clear sky model. These values indicate the maximum values of clearness index measured for a given hour, for all days of month, considering the whole five year period. For instance, the upper value of clearness index for 16 o'clock in June (for 10 minutes time frame) has been registered in June 8, 2003 to 16.10 o'clock. The average values of clearness index are the same for all three time frame database, while the lower values seem obvious to have the higher values for the 60 minutes time frame.

Concerning the fact that some clearness indices are greater than the clearness indices calculated from clear sky model, it can be explained considering the topology and environmental features of area where the laboratory is located. The laboratory is placed near the Mediterranean Sea at a lower altitude in comparison with that of the neighbouring mountains, which surrounds the area. Thus, certainly, the diffuse and reflected components of solar radiation will affect the measured global radiation. Especially at lower solar altitude angle, the global radiation has a high diffuse fraction due to the scattering effects of a greater air mass, this effect being observed especially in first graphic from Figure 4, where the evolution of difference between global and beam radiations in horizontal plane can be observed. Furthermore, the hourly solar radiation data could be really affected, especially due to the reflected component caused by sea reflection, especially near sunrise and sunset, and also by reflection effect of the surrounding mountains, for some period of the year. These effects can be observed from the similar behaviours of clearness index for months characterised by the same solar altitude angle.

In Figure 5, a set of histograms for values of clearness index have been drawn based on 10, 30 and 60 minutes database. As can be seen, the histograms developed based on lower time frames database are characterised by higher values of upper clearness index, the histograms being translated to the right.

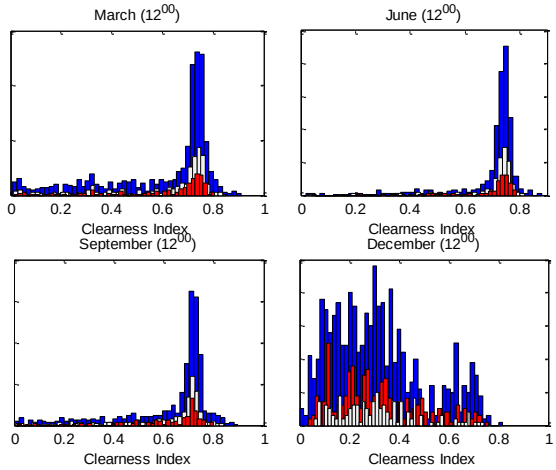

Fig. 5. Comparison of clearness index histograms, at 12^{00} o'clock, on 10 (blue), 30 (white) and 60(red) minutes time frames

In order to evaluate the probability density function of photovoltaic output power, there is required the linear correlation between the hourly diffuse fraction and hourly clearness index [12]. Therefore, from the database, there have been drawn out all values of ration between diffuse and global components, as well as the clearness index, but only between sunrise and sunset hours. Based on these data, the correlation between hourly diffuse fraction and hourly clearness index has been evaluated, as is presented in Figure 6, and for the fitting function it has been found the following linear expression: $k = 1.039 - 1.521 \cdot k_t$.

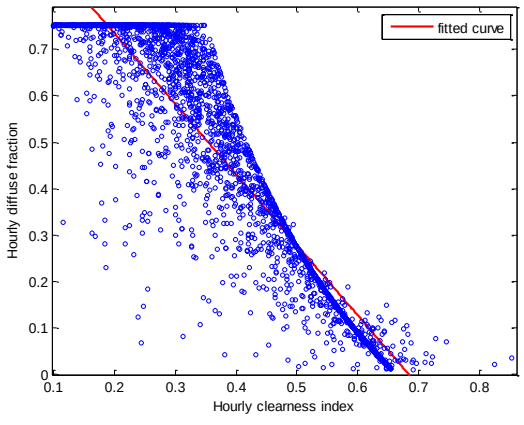

Fig. 6. The linear correlation of hourly diffuse fraction as a function of hourly clearness index

Similar diagrams, like those presented in Figures 1-3, have been plotted for every month of the year, covering the whole five-year period, the clear sky, upper and average values of hourly clearness index, being summarised in Table 1.

Table 1

Hourly clearness index values from clear sky model and from measurement database

		Hour																	
		4	5	6	7	8	9	10	11	12	13	14	15	16	17	18	19	20
Jan.	Clear Sky	0.00	0.00	0.00	0.48	0.67	0.73	0.76	0.77	0.77	0.76	0.73	0.68	0.49	0.00	0.00	0.00	0.00
	$Upper_{10min}$	0.00	0.00	0.00	0.83	0.76	0.82	0.75	0.85	0.86	0.90	0.74	0.75	0.73	0.00	0.00	0.00	0.00
	$Upper_{30min}$	0.00	0.00	0.00	0.75	0.68	0.71	0.72	0.84	0.75	0.72	0.72	0.73	0.62	0.00	0.00	0.00	0.00
	$Upper_{60min}$	0.00	0.00	0.00	0.53	0.65	0.70	0.72	0.78	0.70	0.67	0.66	0.58	0.41	0.00	0.00	0.00	0.00
	Average	0.00	0.00	0.00	0.13	0.20	0.24	0.28	0.29	0.31	0.28	0.24	0.20	0.17	0.00	0.00	0.00	0.00
Feb.	Clear Sky	0.00	0.00	0.21	0.63	0.70	0.77	0.79	0.80	0.80	0.79	0.77	0.73	0.64	0.22	0.00	0.00	0.00
	$Upper_{10min}$	0.00	0.00	0.56	0.69	0.74	0.85	0.87	0.91	0.85	0.78	0.83	0.80	0.69	0.58	0.00	0.00	0.00
	$Upper_{30min}$	0.00	0.00	0.41	0.56	0.71	0.75	0.83	0.89	0.80	0.76	0.74	0.71	0.65	0.44	0.00	0.00	0.00
	$Upper_{60min}$	0.00	0.00	0.20	0.40	0.66	0.74	0.77	0.85	0.77	0.75	0.71	0.61	0.50	0.22	0.00	0.00	0.00
	Average	0.00	0.00	0.05	0.20	0.26	0.34	0.43	0.45	0.46	0.37	0.31	0.26	0.19	0.05	0.00	0.00	0.00
Mar.	Clear Sky	0.00	0.05	0.59	0.72	0.78	0.81	0.82	0.83	0.83	0.82	0.81	0.78	0.72	0.60	0.07	0.00	0.00
	$Upper_{10min}$	0.00	0.49	0.69	0.65	0.82	0.81	0.90	0.91	0.91	0.88	0.90	0.83	0.73	0.64	0.50	0.00	0.00
	$Upper_{30min}$	0.00	0.16	0.50	0.61	0.74	0.79	0.85	0.85	0.85	0.85	0.81	0.73	0.61	0.52	0.17	0.00	0.00
	$Upper_{60min}$	0.00	0.08	0.42	0.57	0.69	0.74	0.81	0.80	0.81	0.83	0.80	0.69	0.55	0.50	0.08	0.00	0.00
	Average	0.00	0.01	0.18	0.23	0.34	0.49	0.56	0.58	0.59	0.57	0.48	0.37	0.28	0.20	0.01	0.00	0.00
Apr.	Clear Sky	0.00	0.46	0.70	0.77	0.81	0.83	0.84	0.84	0.84	0.84	0.83	0.81	0.77	0.67	0.46	0.00	0.00
	$Upper_{10min}$	0.00	0.57	0.58	0.74	0.88	0.97	0.91	0.89	0.90	0.92	0.93	0.91	0.90	0.92	0.85	0.00	0.00
	$Upper_{30min}$	0.00	0.35	0.51	0.66	0.79	0.91	0.85	0.84	0.85	0.85	0.89	0.91	0.83	0.73	0.79	0.00	0.00
	$Upper_{60min}$	0.00	0.31	0.42	0.64	0.71	0.83	0.84	0.81	0.81	0.84	0.87	0.78	0.75	0.67	0.60	0.00	0.00
	Average	0.00	0.11	0.17	0.26	0.42	0.53	0.57	0.59	0.60	0.60	0.58	0.46	0.36	0.30	0.17	0.00	0.00
May	Clear Sky	0.14	0.64	0.74	0.80	0.82	0.84	0.85	0.85	0.85	0.85	0.84	0.82	0.80	0.72	0.64	0.20	0.00
	$Upper_{10min}$	0.53	0.72	0.72	0.82	0.88	0.85	0.86	0.89	0.86	0.87	0.89	0.87	0.89	0.94	0.72	0.73	0.00
	$Upper_{30min}$	0.28	0.48	0.63	0.73	0.80	0.80	0.82	0.86	0.84	0.84	0.84	0.82	0.84	0.79	0.65	0.27	0.00
	$Upper_{60min}$	0.14	0.46	0.55	0.67	0.74	0.78	0.79	0.83	0.83	0.79	0.78	0.77	0.69	0.77	0.58	0.13	0.00
	Average	0.03	0.21	0.27	0.38	0.54	0.60	0.62	0.63	0.64	0.63	0.62	0.58	0.45	0.32	0.27	0.04	0.00
Jun.	Clear Sky	0.33	0.67	0.73	0.80	0.83	0.84	0.85	0.85	0.85	0.85	0.84	0.83	0.80	0.73	0.67	0.34	0.00
	$Upper_{10min}$	0.61	0.63	0.68	0.81	0.85	0.91	0.85	0.83	0.88	0.86	0.83	0.87	0.92	0.72	0.60	0.59	0.00
	$Upper_{30min}$	0.41	0.54	0.64	0.75	0.79	0.83	0.80	0.82	0.82	0.84	0.79	0.83	0.91	0.64	0.52	0.43	0.00
	$Upper_{60min}$	0.20	0.47	0.58	0.67	0.77	0.78	0.78	0.79	0.79	0.79	0.78	0.79	0.71	0.59	0.46	0.22	0.00
	Average	0.10	0.24	0.35	0.50	0.64	0.68	0.69	0.70	0.70	0.68	0.66	0.63	0.51	0.35	0.25	0.11	0.00
Jul.	Clear Sky	0.27	0.65	0.75	0.80	0.83	0.84	0.85	0.85	0.85	0.85	0.84	0.83	0.80	0.74	0.66	0.28	0.00
	$Upper_{10min}$	0.73	0.86	0.90	0.95	0.93	0.90	0.88	0.91	0.85	0.87	0.87	0.84	0.90	0.69	0.55	0.71	0.00
	$Upper_{30min}$	0.37	0.69	0.81	0.93	0.90	0.87	0.84	0.84	0.84	0.79	0.80	0.78	0.83	0.61	0.55	0.35	0.00
	$Upper_{60min}$	0.18	0.59	0.68	0.86	0.90	0.85	0.82	0.83	0.78	0.79	0.78	0.75	0.82	0.58	0.50	0.18	0.00
	Average	0.07	0.25	0.34	0.53	0.68	0.69	0.71	0.70	0.70	0.67	0.65	0.62	0.50	0.28	0.19	0.06	0.00
Aug.	Clear Sky	0.00	0.58	0.72	0.78	0.82	0.84	0.84	0.85	0.85	0.84	0.84	0.82	0.78	0.72	0.59	0.05	0.00
	$Upper_{10min}$	0.00	0.54	0.75	0.79	0.80	0.81	0.80	0.81	0.82	0.84	0.86	0.82	0.74	0.72	0.64	0.74	0.00
	$Upper_{30min}$	0.00	0.48	0.69	0.70	0.78	0.77	0.78	0.79	0.79	0.77	0.80	0.73	0.71	0.64	0.43	0.25	0.00
	$Upper_{60min}$	0.00	0.32	0.66	0.69	0.72	0.76	0.76	0.79	0.79	0.75	0.79	0.71	0.68	0.59	0.34	0.12	0.00
	Average	0.00	0.18	0.41	0.49	0.58	0.62	0.64	0.67	0.67	0.66	0.65	0.61	0.52	0.41	0.21	0.01	0.00
Sept.	Clear Sky	0.00	0.18	0.65	0.75	0.79	0.82	0.83	0.84	0.84	0.83	0.82	0.80	0.72	0.62	0.21	0.00	0.00
	$Upper_{10min}$	0.00	0.48	0.56	0.78	0.82	0.82	0.90	0.89	0.90	0.88	0.90	0.80	0.93	0.55	0.68	0.00	0.00
	$Upper_{30min}$	0.00	0.30	0.48	0.65	0.72	0.77	0.81	0.86	0.84	0.82	0.81	0.74	0.85	0.47	0.37	0.00	0.00
	$Upper_{60min}$	0.00	0.15	0.37	0.59	0.69	0.74	0.78	0.79	0.80	0.80	0.80	0.68	0.71	0.43	0.18	0.00	0.00
	Average	0.00	0.04	0.23	0.32	0.46	0.56	0.61	0.61	0.62	0.62	0.57	0.49	0.33	0.20	0.04	0.00	0.00
Oct.	Clear Sky	0.00	0.00	0.41	0.68	0.75	0.79	0.81	0.81	0.81	0.81	0.79	0.75	0.68	0.42	0.00	0.00	0.00
	$Upper_{10min}$	0.00	0.00	0.57	0.75	0.78	0.92	0.87	0.89	0.91	0.88	0.88	0.82	0.65	0.98	0.00	0.00	0.00
	$Upper_{30min}$	0.00	0.00	0.39	0.60	0.67	0.82	0.81	0.80	0.83	0.79	0.78	0.78	0.55	0.57	0.00	0.00	0.00
	$Upper_{60min}$	0.00	0.00	0.28	0.57	0.64	0.70	0.81	0.78	0.76	0.75	0.71	0.69	0.52	0.28	0.00	0.00	0.00
	Average	0.00	0.00	0.10	0.24	0.31	0.41	0.47	0.53	0.53	0.50	0.45	0.34	0.25	0.11	0.00	0.00	0.00
Nov.	Clear Sky	0.00	0.00	0.04	0.58	0.69	0.75	0.77	0.78	0.78	0.77	0.75	0.70	0.58	0.05	0.00	0.00	0.00
	$Upper_{10min}$	0.00	0.00	0.66	0.61	0.68	0.76	0.82	0.81	0.83	0.82	0.84	0.72	0.93	0.38	0.00	0.00	0.00
	$Upper_{30min}$	0.00	0.00	0.22	0.48	0.54	0.74	0.75	0.77	0.78	0.77	0.71	0.67	0.56	0.13	0.00	0.00	0.00
	$Upper_{60min}$	0.00	0.00	0.11	0.43	0.52	0.64	0.73	0.75	0.76	0.73	0.69	0.65	0.45	0.06	0.00	0.00	0.00
	Average	0.00	0.00	0.01	0.16	0.21	0.29	0.34	0.34	0.35	0.34	0.31	0.25	0.18	0.01	0.00	0.00	0.00
Dec.	Clear Sky	0.00	0.00	0.00	0.35	0.65	0.72	0.75	0.76	0.76	0.75	0.72	0.66	0.36	0.00	0.00	0.00	0.00
	$Upper_{10min}$	0.00	0.00	0.00	0.78	0.67	0.72	0.73	0.72	0.82	0.82	0.85	0.69	0.79	0.00	0.00	0.00	0.00
	$Upper_{30min}$	0.00	0.00	0.00	0.57	0.53	0.66	0.69	0.71	0.76	0.81	0.78	0.64	0.55	0.00	0.00	0.00	0.00
	$Upper_{60min}$	0.00	0.00	0.00	0.30	0.45	0.63	0.68	0.70	0.74	0.73	0.72	0.61	0.38	0.00	0.00	0.00	0.00
	Average	0.00	0.00	0.00	0.11	0.20	0.24	0.27	0.30	0.31	0.31	0.29	0.22	0.11	0.00	0.00	0.00	0.00

4. NUMERICAL ANALYSIS

This section focuses on a numerical evaluation of adequacy indices associated to a grid-connected photovoltaic system designed to supply a load profile. The adequacy indices are obtained by convolving the probability density function of hourly output power of photovoltaic system and probability density function of hourly demanded load. It should be noted that the probability density function of hourly output power is affected only by the upper and average values of hourly clearness index, which means that different probability density functions are obtained for each above database.

In order to check the accuracy of these probability density functions, the monthly daily average irradiation falling on an horizontal surface have been estimated. Thus, the monthly daily average irradiation could be evaluated as the sum of global irradiations on horizontal surface available on original database, or taking in account the mean values of probability density functions of monthly hourly output power, considering a 100% conversion efficiency. Therefore, considering the probability density function from equation (1) with upper values of clearness index from 10, 30 and 60 minutes time frame database, from Holland and Huget hypothesis ($k_{tu}=0.864$) [6] and, also, from clear sky model, the monthly daily average irradiation have been calculated and summarized in Table 2. As a reference, the sum of global irradiation has been also calculated.

Table 2

Monthly daily average irradiation (kWh/m^2/day)

Month	Monthly daily average irradiation based on					
	Global radiation	10 min frame	30 min frame	60 min frame	Holland Huget	Clear sky
January	1.002	1.020	1.018	1.017	1.022	1.018
February	1.967	1.966	1.964	1.963	1.970	1.964
March	3.646	3.595	3.594	3.593	3.596	3.594
April	4.716	4.838	4.836	4.835	4.837	4.835
May	6.046	6.101	6.099	6.098	6.101	6.099
June	7.035	7.064	7.063	7.063	7.065	7.063
July	7.010	6.782	6.781	6.781	6.783	6.782
August	6.067	5.994	5.993	5.993	5.995	5.994
September	4.363	4.279	4.277	4.276	4.280	4.278
October	2.824	2.643	2.638	2.636	2.642	2.637
November	1.274	1.308	1.305	1.304	1.308	1.305
December	0.871	0.973	0.971	0.970	0.976	0.970
Yearly Daily Avg.	3.902	3.881	3.878	3.877	3.880	3.878

As can be seen, the most accurate estimation of monthly daily average irradiation is obtained considering the 10 minutes frame database, but the difference between monthly daily average values calculated based on different database are very small. Consequently, the achieved results establish that the previous probability density functions are correctly evaluated.

Considering the original database, the annual amount of global solar irradiation on horizontal surface is 1441.9 kWh/m^2, which means that for one square meter of a photovoltaic panel with an efficiency around 12%, the annual energy that can be produced is around 173.03 kWh. This annual energy produced by the photovoltaic system can supply different load profiles. Thus, in the paper, in order to consider the load profile on the adequacy indices, three types of load profiles with the same annual energy (173.03 kWh) have been used. For each load profile, the load factor (k_L) has been calculated. The first load profile has been considered to be a smooth load profile with same hourly average values, around 19.75 W and a load factor equal with 100%. The second load profile has been considered to have also a smooth profile, but only for daily hours (i.e. between 6 and 18 o'clock). For this profile, the hourly average values are around 36.47 W, with a load factor 54.16%. The third load profile has been considered to be composed from a base smooth profile for the entire day, with about 10% from daily average load, and the rest of energy has been distributed so as to reach a peak of load at midday, the peak values reaching 37.53 W and a load factor 52.63%. For all three profiles, the values of the demanded load have been thought to be uniformly distributed in an interval with a standard deviation equal with 5%. Thus, the lower and upper values of load are evaluated for each load profile, in accordance with equation (2). Figure 7 depicts the daily load characteristics for all three cases of load profiles, the daily as well as the annual energy demanded being the same in all three cases.

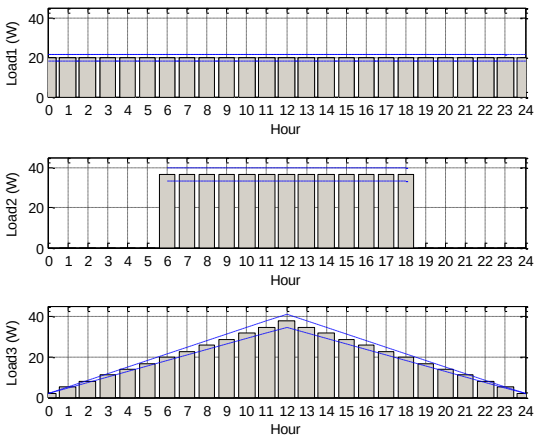

Fig. 7. Daily load profiles: hourly average values (bar graph) and variation intervals (dotted lines)

Based on the above probability density functions, the adequacy indices, for a grid-connected photovoltaic system with one square meter surface and designed to supply above load profiles, have been evaluated as the sum of the hourly adequacy values. The hourly values have been computed using convolution technique, more details about this technique being reported in [14]. For instance, Figure 8 shows the effect of different time frames database on the cumulative distribution functions of generated power. As can be seen, the time frames database change the shape and the scale features of cumulative distribution functions, leading to different results for different load profiles.

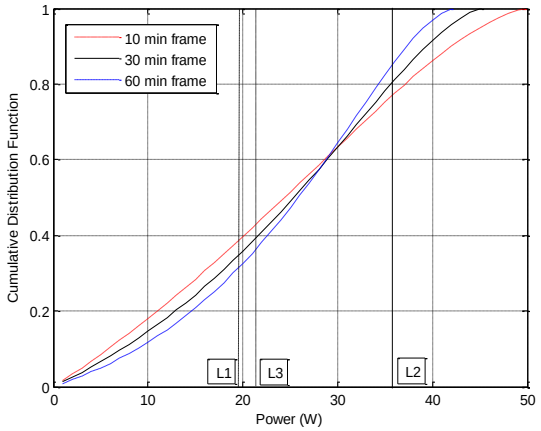

Fig. 8 Cumulative distribution functions of generated power for 10, 30 and 60 minutes time frame database

Table 3 indicates the values of adequacy indices, namely the LOLE (hour/year) and LOEE (kWh/year), considering the upper values of clearness index from above three frame database, the upper value suggested by Holland and Huget and, also, the value of clearness index calculated in the hypothesis of clear sky model.

Table 3

Adequacy indices for different values of upper hourly clearness index and different load profiles

Load profile	Adequacy indices	The upper hourly clearness index from:				
		10 min frame	30 min frame	60 min frame	Holland Huget	Clear sky
Profile 1 (19.75W) k_L=1	LOLE (hour/year)	5930	5920	5910	5930	5920
	LOEE (kWh/year)	116.78	116.68	116.61	116.81	116.69
Profile 2 (36.47W) k_L=0.542	LOLE (hour/year)	1995	1978	1966	2001	1981
	LOEE (kWh/year)	70.760	70.439	70.203	70.872	70.492
Profile 3 (37.53W) k_L=0.526	LOLE (hour/year)	5871	5857	5847	5876	5859
	LOEE (kWh/year)	84.459	84.233	84.074	84.536	84.264

From Table 3 it can be observed that the adequacy indices strongly depend on the load profiles. For first and third load profiles, the LOLE index values are very high, especially due to the demanded load during the nightly hours, when the grid-connected photovoltaic system is characterised by a lack of generated power. For these load profiles, about 4380h from LOLE index values are due to the lack of generated power during the night. Instead, the second load profile, characterised by load values only for the daily hours, leads to relatively small values of LOLE index.

As can be seen, the nightly load values of first and third load profiles affect in similar manner the LOLE indices, while they significantly affect, with different weights, the LOEE indices. Thus, the first profile, compared with the third profile, causes higher values of LOEE because, during the night, a significant amount of energy is not served. It is noted that the lower values of adequacy indices are registered for second profile. This is due to the fact that the second load profile presents a regular distribution during the daily hours, when the demanded load is covered by the generated power profile.

For the same load profile, it can be observed that the adequacy indices have fairly close values, the results depending on the database used to evaluate the upper values of clearness index. The lower values of range of LOLE and LOEE indices are registered for 60 minutes frame database, while the upper indices are recorded for upper value of clearness index suggested by Holland and Huget (k_{tu}=*0.864*). Although, at first sight it might seem obvious that the maximum values to be registered for clear sky model, the adequacy indices from Holland and Huget hypothesis are higher than from clear sky model, because the *0.864* value has been considered as the maximum value for all hours and months of the year, while the clear sky model, as presented in Table 1, presents values close to *0.864* only in the summer months and only around the noon hours.

Considering that the values of adequacy indices are close, it can be concluded that using the upper value of clearness index, suggested by Holland and Huget, together with the average values of clearness index from an hourly registered database, a sufficiently good estimation of adequacy indices could be obtained.

5. CONCLUSIONS

This study has been developed in order to evaluate the effect of different time frames database on the probabilistic behaviour of a grid-connected

photovoltaic system, designed to supply a power with a given profile. Thus, a 10 minutes time frame database, collected on Ajaccio (Corsica, France), has been involved in order to evaluate what happens when the time sampling is reduced from hourly to intra-hourly time frame intervals.

The first conclusion of this paper is that the load profile has the highest influence on the adequacy indices. Consequently, a design of a photovoltaic system based on demanded load profile is essential to reduce the adequacy indices of a grid-connected photovoltaic system. It seems interesting for future works to develop a model to manage/choose a suitable hourly load profile for a grid-connected photovoltaic system.

The second conclusion is that the accuracy of adequacy indices is not highly dependent on the database. Thus, in the paper a study of the influence of different time frame database on the adequacy indices has been carried out. Nevertheless, the adequacy indices over different time frames have given very close results, therefore it is difficult to indicate the best database to calculate the adequacy indices. However, considering the upper value of clearness index, suggested by Holland and Huget, together with the average values of clearness index from a hourly registered database, could lead to a sufficiently good estimation of adequacy indices.

Acknowledgement

This paper was supported by the project PERFORM-ERA 'Postdoctoral Performance for Integration in the European Research Area' (ID-57649), financed by the European Social Fund and the Romanian Government.

BIBLIOGRAPHY

[1] **Billinton R., Allan R.** *Reliability evaluation of power systems*, 2nd Edition, Plenum Press, NewYork, 1996.

[2] **Endrenyi J.** *Reliability modelling in electric power systems*, Wiley and Sons, NewYork, 1978.

[3] **Tina G., Gagliano S., Raiti S.** *Hybrid solar/wind power system probabilistic modelling for long-term performance assessment* Solar Energy, vol. 80, 2006, pp. 578–588.

[4] **Tina G. M., Gagliano S.** *Probabilistic modelling of hybrid solar/wind power system with solar tracking system*, Renewable Energy vol. 36, 2011, pp. 1719-1727.

[5] **Conti S., Crimi T., Raiti S., Tina G., Vagliasindi U**. *Probabilistic approach to assess the performance of grid-connected PV systems*, Proceedings of 7th International Conference on Probabilistic Methods Applied to Power Systems, Naples, Italy, September 2002.

[6] **Hollands K. T., Huget R. G.** *A Probability Density Function for the clearness index, with applications*. Solar Energy vol. 30, 1983, pp. 195-209.

[7] **Notton G., Poggi P., Cristofari C.** *Predicting hourly solar irradiations on inclined surfaces based on the horizontal measurements: Performances of the association of well-known mathematical models*, Energy Conversion and Management, vol. 47, 2006, pp. 1816–1829.

[8] **Notton G., Cristofari C., Poggi P.** *Performance evaluation of various hourly slope irradiation models using Mediterranean experimental data of Ajaccio*, Energy Conversion and Management, vol. 47, 2006, pp. 147–173.

[9] **Notton G., Cristofari C., Muselli M., Poggi P.** *Calculation on an hourly basis of solar diffuse irradiations from global data for horizontal surfaces in Ajaccio* Energy Conversion and Management, vol. 45, 2004, pp. 2849–2866.

[10] **Rigollier C., Bauer O., Wald L.** *On the clear sky model of the 4th European Solar Radiation Atlas with respect to the Heliosat method* Solar Energy, vol. 68, 2000, pp. 33-48.

[11] **Scharmer K., Greif J.** *The European Solar Radiation Atlas, Vol. 1: Fundamentals and maps*, Les Presses de l'École des Mines, Paris, 2000.

[12] **Perpiñana O., Lorenzob E. Castroc M.A., Eyrasa R.** *On the complexity of radiation models for PV energy production calculation*, Solar Energy, volume 82, issue 2, February 2008, pp. 125–131.

[13] **Barbaro S., Cannata G., Coppolino S., Leone C., Sinagra E.** *Diffuse Solar radiation statistics for Italy*, Solar Energy, vol. 26, 1981, pp. 429-435.

[14] **Nemeș C., Munteanu F.** *A probabilistic model for power generation adequacy evaluation*, Revue Roumaine des Sciences Techniques, Série Électrotechnique et Énergétique, Tome 56, Issue 1, 2011, pp. 36-46.

About the authors

Prof. **Giuseppe Marco TINA,** PhD.
Technical University of Catania, Italy,
email: Giuseppe.tina@dieei.unict.it

Giuseppe M. Tina (M'97) received his M.Sc. (1988) and the Ph.D. degree (1992) both in Electrical Engineering from the University of Catania. He joined Agip Refineries and ST Microelectronics (Italy) where he worked as Electrical Engineer. He is now Associate Professor in the Dept. of Electrical, Electronics and System Engineering at the University of Catania. His research interests include renewable generation systems, especially wind and photovoltaic systems, Dispersed Generation Systems, ancillary services market and storage systems. He is in charge of IDRILAB research laboratory ("LABoratory for Renewable Hydrogen").

Prof. **Gilles NOTTON**, PhD.
University of Corsica, France,
email: notton@univ-corse.fr

Gilles Notton gained Ph.D degrees in Energy Engineering in 1992 from the University of Corsica (France). He obtained its accreditation to supervise research in 2002. He is working in the fields of renewable energy for over 20 years. Since 2003, he was responsible of a research network on renewable energy systems between France and Oriental and Central European Countries with the support of the French Environment and Energy Management Agency (ADEME). His research interests cover renewable energy sources estimations, Wind/PV hybrid systems and development of new concepts of solar collector with high integration level in building. His career's output includes over 40 international publications and one hundred communications in international congresses.

Lecturer **Ciprian NEMES**, PhD.
Technical University of Iasi Romania, Faculty of Electrical Engineering.
email:cnemes@ee.uiasi.ro

Ciprian Nemes received the M.Sc degree in Electrical Engineering and Ph.D degree in Reliability Engineering, from "Gh. Asachi" Technical University of Iasi, Romania, in 1998 and 2005, respectively. Since 1998, he has been with Faculty of Electrical Engineering, Technical University of Iasi, where currently he is a Senior Lecturer. He is now involved in a postdoctoral research project, this paper being carried out during the postdoctoral research stage of the Dr. Nemes in IDRIDLab, University of Catania, Italy. His current research interests are in the area of adequacy assessment of electrical power systems, power system planning based on risk assessment, renewable energy sources operation and their planning.